

Probabilities as a bridge between classical and quantum-mechanical treatments

Lorenzo J Curtis and David G Ellis

Department of Physics and Astronomy, University of Toledo, Toledo, OH 43606, USA

E-mail: ljc@physics.utoledo.edu and dge@physics.utoledo.edu

Received 19 May 2005, in final form 19 January 2006

Published 28 February 2006

Online at stacks.iop.org/EJP/27/485

Abstract

There are significant differences in the structures of course presentations of classical mechanics and quantum mechanics, but also essential links that connect the two approaches. A large part of the differences in approach do not involve quantization, but rather the traditional use of instantaneous values to describe macroscopic objects and position probability densities to describe microscopic objects. A pedagogic reformulation of the classical problem to bridge this gap is presented here. The method is numerical in nature, but for illustrative purposes it is herein applied to two specific cases for which analytic solutions also exist, the Kepler–Coulomb potential and the isotropic harmonic oscillator. Using this approach, classical systems can be examined in the presence of perturbations in the same way as is used in quantum mechanics courses. Semiclassical quantization can also be introduced to extend the connection to a quantum-mechanical treatment.

1. Introduction

Traditional approaches to the teaching of classical mechanics and quantum mechanics contain both supportive connections and significant distinctions. Classical mechanics extends the elementary Newtonian concepts to the Lagrangian and Hamiltonian formulations, to the least action principle, to the angle-action variables, etc, in ways that are the essential framework of quantum mechanics. However, there are significant distinctions between the two approaches that arise not because of quantization, but rather from the nonessential tendency to describe macroscopic systems by instantaneous values for position, speed and acceleration, and microscopic systems by time-averaged position probability densities.

The reasons for this are clear, since a macroscopic classical trajectory is disturbed only slightly when successively interrogated with visible light, whereas a microscopic system may be destroyed by interrogation with a single short-wavelength photon. Thus the description

of the microscopic quantum system requires the superposition of many similarly interrogated systems. We suggest here a way of incorporating classical position probability densities into courses in both classical mechanics and quantum mechanics which provides a useful pedagogic bridge between the two.

Although the traditional tracking of instantaneous positions (like a series of snapshots) has conceptual advantages, the use of position probabilities (like a time exposure that reveals motion through the degree of overexposure) has other advantages. It allows macroscopic and microscopic objects to be studied by similar techniques [1]. It is easily extended to include many-body interactions, since the probability distributions can be superimposed [2]. For example, although Newton's formulation of the motion of a single planet used instantaneous values, in Gauss's formulation of the mutual perturbations of planets he replaced each planet by a uniform circular ring of the same mass and orbital radius [3]. This was clearly an early analogue of a position probability density formulation. Another advantage of the probabilistic approach is that it provides a convenient way of performing numerical computations for potentials that do not have an analytic solution.

A formulation is presented here in which the three-dimensional motion of a particle in a central potential is treated in terms of classical position probability densities along the radial coordinate. The approach is quite general and can be applied numerically to an arbitrary potential for which no analytic solution is given. However, as an example of the approach, the method is here applied to two potentials for which analytic solutions exist, the Kepler–Coulomb problem and the isotropic harmonic oscillator. In this manner, the specific values obtained from the numerical solution can be compared with the formulae deduced from the analytic solution.

These two potentials are frequently encountered in introductory quantum mechanics courses. Although these two lead to solutions that possess certain symmetries, they also have interesting differences. For example, the Kepler–Coulomb exemplifies an interaction that decreases with increasing separation, whereas the isotropic harmonic oscillator exemplifies an interaction that increases with increasing separation.

In this presentation, the classical equations for the radial distribution and various expectation values will first be developed. These equations will then be solved numerically for specific values of the energies and angular momenta. These solutions will then be compared with formulae obtained by incorporating the known orbit equations into the formulation. The results will then be applied to treat various possible perturbations to these systems. Finally, the connection to the quantum-mechanical solution will be examined in context of the EBK semiclassical quantization of action.

2. Radial distributions for central potentials

Consider a particle of mass m bound by a central potential $V(r)$ described by the standard spherical polar coordinates r, θ, φ . By the standard methods of classical mechanics this leads to a Lagrangian

$$L = \frac{1}{2}m(\dot{r}^2 + r^2\dot{\theta}^2 + r^2 \sin^2 \theta \dot{\varphi}^2) - V(r). \quad (1)$$

This yields the generalized momenta

$$p_r = \frac{\partial L}{\partial \dot{r}} = m\dot{r}, \quad p_\theta = \frac{\partial L}{\partial \dot{\theta}} = mr^2\dot{\theta}, \quad p_\varphi = \frac{\partial L}{\partial \dot{\varphi}} = mr^2 \sin^2 \theta \dot{\varphi}. \quad (2)$$

Since the potential is independent of angular variables, the total angular momentum L is independent of time, and can be demonstrated by the Hamilton–Jacobi method to be given by

$$L^2 = p_\theta^2 + p_\varphi^2 / \sin^2 \theta = \text{constant}. \quad (3)$$

Furthermore the motion is confined to a plane, which we take as the $\theta = \pi/2$ plane, and geometrical considerations lead to the well-known result that equal areas are swept out in equal times

$$\frac{1}{2}r^2 \frac{d\varphi}{dt} = \frac{A}{T} = \frac{L}{2m} \quad (4)$$

where T is the period of the angular motion and A is the area enclosed by the orbit. Although Kepler's second law was originally formulated for the inverse square law, it is valid for any central potential. The area enclosed by the orbit does, however, depend on $V(r)$.

In terms of these quantities, the total energy of the system is given by

$$E = \frac{p_r^2}{2m} + \frac{L^2}{2mr^2} + V(r). \quad (5)$$

At this point in the development, the standard approach in classical mechanics would be to obtain the Lagrange equation for the time dependence of the radial coordinate, and deduce from it the orbital equation that relates r and φ . In contrast, the quantum-mechanical approach would account for both the radial and angular motions by mapping the radial distribution. A classical analogue of this approach can be obtained by computing the differential fraction $P(r) dr$ of the time spent at each radial distance r (in accordance with the correspondence limit of the quantum-mechanical formulation [4]). Note that even though the quantum-mechanical treatment is three dimensional, the radial probability distribution $P(r) dr$ has exactly the same meaning in both treatments: the probability of finding the particle at a distance between r and $r + dr$ of the origin.

For a closed orbit, the angular rotation period T must be an integer multiple N of the radial libration period ($N = 1$ for the Kepler–Coulomb problem; $N = 2$ for the isotropic harmonic oscillator), and this quantity is given by

$$P(r) dr = \frac{2N dt}{T} = \frac{2N}{T} \frac{dr}{dr/dt} = \frac{2Nm dr}{T p_r}. \quad (6)$$

The object will thus undergo librations between the distances of closest approach A_- and of greatest recession A_+ , traversing the interval $2N$ times. Here we have used the radial speed (and thus the radial momentum) to convert from time to space coordinates, but the radial distribution remains a time average and not a space average.

However, the restriction to closed orbits is very confining and not essential if the normalization of $P(r)$ is made through numerical integration from A_- to A_+ on a precessing orbit. In this case, the normalizing constant C that replaces the closed orbit constant $2Nm/T$ in

$$P(r) dr = C dr/p_r \quad (7)$$

can be obtained through numerical integration of

$$P(r) dr = \frac{dr}{p_r(r)} \left[\int_{A_-}^{A_+} \frac{dr'}{p_r(r')} \right]^{-1} \quad (8)$$

irrespective of any knowledge of the orbital or radial periods.

The radial distribution is thus given by the reciprocal of the radial momentum, which for a given potential is prescribed through equation (5) to be

$$p_r/\sqrt{2m} = \sqrt{E - V(r) - L^2/2mr^2}. \quad (9)$$

Combining equations (7) and (9), the radial distribution can be obtained from

$$P(r) dr = C \frac{dr}{\sqrt{E - V(r) - L^2/2mr^2}}. \quad (10)$$

Values for $P(r)$ are obtained from equation (10) for specific values of E and L and a range of numerical values for r and $V(r)$: the normalized distribution is obtained using equation (8).

For given numerical choices of E and L , any numerical array can be inserted for $V(r)$, and from it a radial distribution can be computed. For example, this method could be used to investigate examples such as the Yukawa or the Lennard–Jones 6–12 potential, or a digitized representation of a molecular potential. For these numerical applications, for which there is no simple equation for the orbit locus or its enclosed area, the normalized distribution can be obtained directly from equations (8) and (10).

The classical turning points A_{\pm} in the periodic orbital motion occur where the radial momentum vanishes, specified by the roots of the equation

$$Er^2 - V(r)r^2 - L^2/2m = 0 \quad (11)$$

which can also be found numerically.

Any perturbations to the assumed potential that can be written as a power series in r can be evaluated by computing the average values of powers of r in the unperturbed radial distribution

$$\langle r^k \rangle = \int_{A_-}^{A_+} dr P(r) r^k. \quad (12)$$

3. Numerical solution

3.1. Kepler–Coulomb potential

In this case the potential is of the form

$$V(r) = -\kappa/r. \quad (13)$$

In the classical case, both the energy and the momentum can take on any value, so the numerical solution must choose specific values for these quantities. In order to subsequently compare the numerical results with analytic results, we arbitrarily choose the values corresponding to the 3p level in hydrogen, which has the energy and (semiclassical) angular-momentum values

$$E = -R_y/9, \quad L = 3\hbar/2. \quad (14)$$

Here we use Rydberg energy units R_y and Bohr length units a_0 . These are connected to other units by the relationships $2R_y a_0 = \kappa$ and $2R_y a_0^2 = \hbar^2/m$. In these units, the radial momentum is given by

$$\frac{p_r^2}{2m} = R_y \left[-\frac{1}{9} + \frac{2a_0}{r} - \frac{9a_0^2}{4r^2} \right]. \quad (15)$$

To simplify computation in this section, energies will be here measured in units of R_y and distances in units of a_0 .

Although equation (15) is quadratic and could be solved analytically, in the spirit of this generalized approach the roots were found numerically. To do this, equation (15) was digitized using a preliminary grid in r , and the zero-point crossovers were computed. The range over which $p_r(r)$ is positive was determined to be

$$1.2058 \leq r \leq 16.794. \quad (16)$$

To normalize the distribution, a numerical integration was performed of the quantity

$$P(r) dr = \frac{dr}{C \sqrt{-\frac{1}{9} + \frac{2}{r} - \frac{9}{4r^2}}} \quad (17)$$

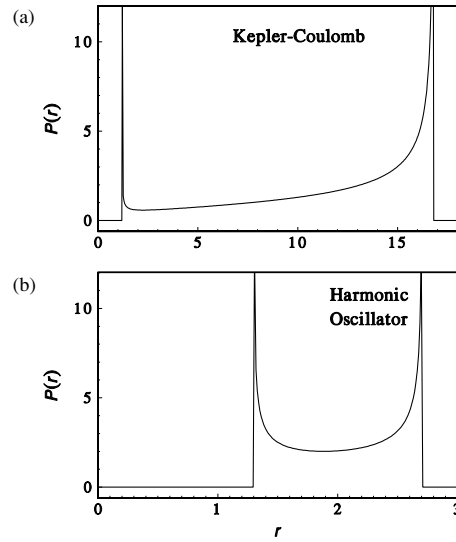


Figure 1. Classical radial distributions for the numerically computed examples.

where C is a normalization factor. A grid of 100 000 points was set up between these limits and a simple rectangular numerical integration was performed. (A trapezoidal integration is inappropriate, since the integrand is unbounded at the endpoints. However, such technical points can also be accounted for automatically by use of a computer package such as Maple or Mathematica.) This yielded the value $C = 84.82$. This value was inserted into the radial probability, which is shown in figure 1(a).

Using this distribution, a selection of average moments were computed by numerical integration of equation (12). This yielded

$$\langle r \rangle = 12.375 \quad \langle r^{-1} \rangle = 0.1111 \quad \langle r^{-2} \rangle = 0.02469 \quad \langle r^{-3} \rangle = 0.01097. \quad (18)$$

These values can be compared with analytical results presented in the subsequent sections.

3.2. Isotropic harmonic oscillator

In this case the potential is of the form

$$V(r) = kr^2/2. \quad (19)$$

Again, in the classical case the possible values of the energy and angular momentum are continuous, but to facilitate later comparison with analytic results, we chose values corresponding to $n_r = 0$ and $\ell = 3$ in the analogous quantum-mechanical problem. Thus

$$E = \frac{9}{2}\hbar\sqrt{\frac{k}{m}}, \quad L = \frac{7}{2}\hbar. \quad (20)$$

The radial momentum is given by

$$\frac{p_r^2}{2m} = \hbar\sqrt{\frac{k}{m}} \left[\frac{9}{2} - \frac{\sqrt{mk}}{\hbar} \frac{r^2}{2} - \frac{\hbar}{\sqrt{mk}} \frac{49}{8r^2} \right]. \quad (21)$$

To simplify computation in this section, energies will be measured in units of $\hbar\sqrt{\frac{k}{m}}$ and lengths in units of $\sqrt{\hbar/\sqrt{mk}}$.

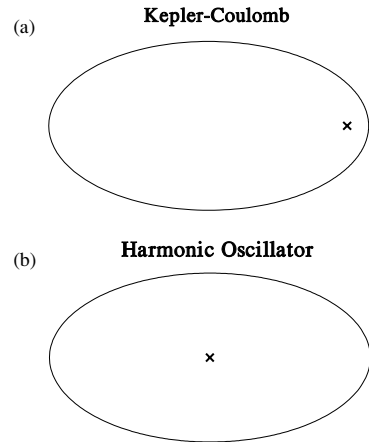


Figure 2. Comparison of the elliptic orbits for the two examples.

This form is also quadratic and analytically solvable, but the roots were found numerically as described above, by digitizing the equation and locating zero-point crossovers. The range over which $p_r(r)$ is positive was determined to be

$$1.2929 \leq r \leq 2.7071. \quad (22)$$

To normalize this distribution, a numerical integration as described above was performed of the quantity

$$P(r) dr = \frac{dr}{C \sqrt{\frac{9}{2} - \frac{r^2}{2} - \frac{49}{8r^2}}}, \quad (23)$$

which yielded a value $C = 2.215$. This value was inserted into the radial probability, which is shown in figure 1(b).

This distribution was also applied to compute a selection of average moments using equation (12). This yielded

$$\langle r^2 \rangle = 4.500, \quad \langle r^4 \rangle = 24.25, \quad \langle r^{-2} \rangle = 0.2857, \quad \langle r^{-4} \rangle = 0.1050. \quad (24)$$

These values can also be compared with analytical results presented in the subsequent sections.

4. Analytic solutions

The classical solutions for both of these examples are well known, and both yield elliptic orbits, with semimajor and semiminor axes denoted henceforth by a and b . In both of these cases, the area subtended by the orbit is given by

$$A = \pi ab. \quad (25)$$

4.1. Kepler–Coulomb orbit

For the Kepler–Coulomb problem, the equation for the ellipse (an example of which is shown in figure 2(a)) is

$$\frac{1}{r} = \frac{1 + \varepsilon \cos \phi}{a(1 - \varepsilon^2)} \quad (26)$$

where ε is the eccentricity

$$\varepsilon = \sqrt{1 - b^2/a^2} \quad (27)$$

with the turning points

$$A_{\pm} = a(1 \pm \varepsilon). \quad (28)$$

For this case the coordinate system is centred on one of the foci of the ellipse. The period of the librations of the radial motion is equal to the period of the rotational motion, so $N = 1$.

The potential

$$V(r) = -\kappa/r \quad (29)$$

gives rise to a total energy

$$E = -\kappa/2a. \quad (30)$$

We define the binding energy $E_B = -E$ as a positive number. The radial momentum is defined through

$$p_r^2/2m = -E_B + \kappa/r - L^2/2mr^2, \quad (31)$$

which has the roots

$$A_{\pm} = \frac{\kappa}{2E_B} \pm \sqrt{\left(\frac{\kappa}{2E_B}\right)^2 - \frac{L^2}{2mE_B}}. \quad (32)$$

From this the semimajor and semiminor axes can be identified as

$$a = \kappa/2E_B, \quad b = L\sqrt{2mE_B}. \quad (33)$$

By factorization of these constants the radial distribution can be written as (with $N = 1$ since here the periapsis and apoapsis are separated by 180°)

$$P(r) dr = \frac{1}{\pi a} \frac{r dr}{\sqrt{(A_+ - r)(r - A_-)}}. \quad (34)$$

4.2. Isotropic harmonic oscillator orbit

For the isotropic harmonic oscillator, the equation of the ellipse (an example of which is shown in figure 2(b)) is [5]

$$\frac{1}{r^2} = \frac{1}{2} \left(\frac{1}{a^2} + \frac{1}{b^2} \right) - \left(\frac{1}{a^2} - \frac{1}{b^2} \right) \cos 2\varphi. \quad (35)$$

In this case, the centre of the ellipse is centred on the origin of the coordinate system, so the turning points are given by

$$A_+ = a, \quad A_- = b. \quad (36)$$

A better comparison with the Kepler–Coulomb problem can be obtained by rewriting equation (35) as

$$\frac{1}{r^2} = \left(\frac{a^2 + b^2}{2a^2b^2} \right) \left[1 + \left(\frac{a^2 - b^2}{a^2 + b^2} \right) \cos 2\varphi \right]. \quad (37)$$

Defining here

$$\varepsilon \equiv \frac{a^2 - b^2}{a^2 + b^2}, \quad (38)$$

which yields

$$\sqrt{1 - \varepsilon^2} = \sqrt{1 - \left(\frac{a^2 - b^2}{a^2 + b^2}\right)^2} = \left(\frac{2ab}{a^2 + b^2}\right), \quad (39)$$

and thus simplifies equation (35) to

$$\frac{1}{r^2} = \frac{1 + \varepsilon \cos 2\varphi}{ab\sqrt{1 - \varepsilon^2}}. \quad (40)$$

Here the radial librations pass through two periods for each period of the angular rotation, hence $N = 2$.

The potential

$$V(r) = kr^2/2 \quad (41)$$

yields the momentum

$$p_r^2/2m = E - kr^2/2 - L^2/2mr^2, \quad (42)$$

which has the roots

$$A_{\pm}^2 = \frac{E}{k} \pm \sqrt{\left(\frac{E}{k}\right)^2 - \frac{L^2}{mk}}. \quad (43)$$

Since the turning points are here at the semimajor and semiminor axes $a = A_+$ and $b = A_-$, it can be seen that

$$\frac{a^2 + b^2}{2} = \frac{E}{k}, \quad ab = \frac{L}{\sqrt{mk}}. \quad (44)$$

Using equation (4), this gives a value for the period

$$T = \frac{2m\pi ab}{L} = 2\pi\sqrt{\frac{m}{k}}. \quad (45)$$

Inserting these relationships into equation (6)

$$P(r) dr = \frac{2}{\pi} \frac{r dr}{\sqrt{(A_+^2 - r^2)(r^2 - A_-^2)}}. \quad (46)$$

The radial distribution density corresponding to the orbit in figure 2(b) is shown in figure 1(b).

5. Expectation values

As shown earlier, average values of quantities weighted by these distributions can be obtained by direct numerical integration of these expressions. However, for the special case of these two analytically specified orbits, it is possible to transform the expressions into the form of the standard integral [6]

$$\frac{1}{2\pi} \int_0^{2\pi} d\varphi (1 + \varepsilon \cos \varphi)^n = (1 - \varepsilon^2)^{n/2} P_n \left(\frac{1}{\sqrt{1 - \varepsilon^2}} \right) \quad (47)$$

where $P_n(x)$ is the Legendre polynomial (in an unusual application where the argument $x > 1$). Negative powers can be handled using the relationship

$$P_{-n}(x) = P_{n-1}(x). \quad (48)$$

To achieve this, note that in addition to the radial integral formulation of equation (12), the expectation value can alternatively be written as

$$\langle r^k \rangle = \frac{1}{T} \int_0^T dt r^k = \frac{1}{T} \int_0^{2\pi} \frac{d\varphi}{d\varphi/dt} r^k. \quad (49)$$

Conservation of angular momentum relates r and φ through equation (4), which can be rewritten as

$$T d\varphi/dt = 2\pi ab/r^2. \quad (50)$$

Inserting this into equation (49)

$$\langle r^k \rangle = \frac{1}{2\pi ab} \int_0^{2\pi} d\varphi r^{k+2}. \quad (51)$$

It remains only to choose the equation of the orbit, and to use equation (47) to evaluate this expectation value.

5.1. Kepler–Coulomb problem

Here the coordinate system is centred on one of the foci of the ellipse, which has the equation

$$\frac{1}{r} = \frac{a}{b^2} (1 + \varepsilon \cos \varphi) \quad (52)$$

where $\varepsilon \equiv \sqrt{1 - b^2/a^2}$ is the eccentricity of the ellipse. Inserting this relationship for r into equation (51)

$$\langle r^k \rangle = \frac{1}{ab} \left(\frac{a}{b^2}\right)^{-k-2} \frac{1}{2\pi} \int_0^{2\pi} d\varphi (1 + \varepsilon \cos \varphi)^{-k-2} \quad (53)$$

which, using equation (47), becomes

$$\langle r^k \rangle = b^k \left(\frac{b}{a}\right) P_{-k-2} \left(\frac{a}{b}\right). \quad (54)$$

A few examples are

$$\begin{aligned} \langle r \rangle &= a[3 - (b/a)^2]/2, & \langle r^{-1} \rangle &= 1/a, & \langle r^{-2} \rangle &= 1/ab, \\ \langle r^{-3} \rangle &= 1/b^3, & \langle r^{-4} \rangle &= \langle r \rangle/b^5. \end{aligned} \quad (55)$$

5.2. Isotropic harmonic oscillator problem

Here the equation of the ellipse of the form

$$\frac{1}{r^2} = \left(\frac{a^2 + b^2}{2a^2b^2}\right) (1 + \varepsilon \cos 2\varphi). \quad (56)$$

The expectation value is thus given by

$$\langle r^k \rangle = \frac{1}{ab} \left(\frac{a^2 + b^2}{2a^2b^2}\right)^{-\frac{k+2}{2}} \frac{1}{2\pi} \int_0^{2\pi} d\varphi (1 + \varepsilon \cos 2\varphi)^{-\frac{k+2}{2}} \quad (57)$$

which integrates to

$$\langle r^k \rangle = (ab)^{k/2} P_{-\frac{k+2}{2}} \left(\frac{a^2 + b^2}{2ab}\right). \quad (58)$$

This result is valid for both odd and even powers. For odd powers, the Legendre function can be evaluated numerically as a hypergeometric series, as shown in the appendix.

A few examples are

$$\begin{aligned} \langle r^2 \rangle &= (a^2 + b^2)/2 & \langle r^4 \rangle &= [3(a^2 + b^2)^2 - 4a^2b^2]/8 \\ \langle r^{-2} \rangle &= 1/ab & \langle r^{-4} \rangle &= (a^2 + b^2)/2a^3b^3. \end{aligned} \quad (59)$$

6. Perturbation calculations

One of the strengths of this method is the ease with which perturbations to the energy of the system can be computed. The total unperturbed energy can be written in terms of powers of r by deducing the average kinetic energy from the potential using the virial theorem ([7], p 85)

$$\begin{aligned} E &= \langle KE \rangle + \langle V(r) \rangle \\ &= \frac{1}{2} \left\langle r \frac{dV}{dr} \right\rangle + \langle V(r) \rangle. \end{aligned} \quad (60)$$

The total energy E' in the presence of an additional perturbation of the form $\Delta V(r)$ can be computed as

$$E' = E + \langle \Delta V(r) \rangle. \quad (61)$$

6.1. Example 1: Kepler–Coulomb with a $1/r^3$ perturbation

This can occur, for example, in an atom with a spin–orbit magnetic interaction, or in a gravitational system with a Schwarzschild general relativistic correction ([7], p 511).

The energy of the system is

$$E = \langle -\kappa r^{-1} \rangle + \frac{1}{2} \langle \kappa r^{-1} \rangle \quad (62)$$

If the perturbation is $\Delta V(r) = \lambda/r^3$, the perturbed energy is

$$\begin{aligned} E' &= -\frac{\kappa}{2} \langle r^{-1} \rangle + \lambda \langle r^{-3} \rangle \\ &= -\frac{\kappa}{2a} + \frac{\lambda}{b^3} \end{aligned} \quad (63)$$

which results in a precession of the ellipse.

6.2. Example 2: anharmonic oscillator with an r^4 perturbation

The energy of the system is

$$E = \left\langle \frac{1}{2} \kappa r^2 \right\rangle + \left\langle \frac{1}{2} \kappa r^2 \right\rangle. \quad (64)$$

If the perturbation is $\Delta V(r) = \lambda r^4$, the perturbed energy is

$$\begin{aligned} E' &= k \langle r^2 \rangle + \lambda \langle r^4 \rangle \\ &= \frac{k}{2} (a^2 + b^2) + \frac{\lambda}{4} [3(a^2 + b^2)^2 - 2a^2 b^2] \end{aligned} \quad (65)$$

which also results in a precession of the ellipse.

7. The semiclassical EBK quantization

In the classical considerations above, E and L were assumed to take on a continuum of values, and the probability was computed from the momentum for arbitrary choices of these quantities. However, for bound states, first quantization (beginning with the semiclassical Bohr–Sommerfeld–Wilson (BSW) rule) restricts E and L to values for which the action integral corresponds to integer multiples of \hbar . There were mathematical shortcomings in the original BSW formulation in the presence of caustics (turning points), but these were overcome in

reformulations by Einstein–Brillouin–Keller (EBK) [1]. The semiclassical EBK quantization rule is given by

$$\left(n_i + \frac{\mu}{4}\right) = \oint dq_i p_i, \quad (66)$$

where μ is the Maslov index, which counts the number of turning points. This formalism was used to compute the quantized values for E and L in an earlier paper [8], and these results can be related to the semimajor and semiminor axes of the elliptic orbits through equations developed above. The angular phase integrals yield a value for the angular momentum

$$L = (\ell + 1/2)\hbar. \quad (67)$$

Note that the square of this result $L^2 = [\ell(\ell + 1) + 1/4]\hbar^2$ agrees with the quantum-mechanical result in the correspondence limit.

7.1. Kepler–Coulomb

The EBK result [8] for this energy is given by

$$E_B = \frac{m\kappa^2}{2\hbar^2} \frac{1}{(n_r + \ell + 1)^2}. \quad (68)$$

Substituting equations (67) and (68) into equations (33)

$$a = \frac{\kappa}{2E_B} = \frac{\hbar^2}{m\kappa} (n_r + \ell + 1)^2, \quad b = \frac{L}{\sqrt{2mE_B}} = \frac{\hbar^2}{m\kappa} (n_r + \ell + 1) \left(\ell + \frac{1}{2}\right). \quad (69)$$

These results can be used with the expressions in section 5.1 to make comparisons with the numerical calculations of section 3.1 (with $n_r = \ell = 1$), and to obtain explicit formulae for the perturbations in section 6.1.

7.2. Isotropic harmonic oscillator

From [8], the EBK result for this energy is given by

$$E = \hbar \sqrt{\frac{k}{m}} (2n_r + \ell + 3/2). \quad (70)$$

Use of equation (44) yields

$$\frac{a^2 + b^2}{2} = \frac{E}{k} = \frac{\hbar}{m\omega} \left(2n_r + \ell + \frac{3}{2}\right) \quad ab = \frac{L}{\sqrt{mk}} = \frac{\hbar}{m\omega} \left(\ell + \frac{1}{2}\right). \quad (71)$$

These results can be used with the expressions in section 5.2 to make comparisons with the numerical calculation of section 3.2 (with $n_r = 0$ and $\ell = 3$), and to obtain explicit expressions for the perturbations in section 6.2.

8. Conclusion

These examples of an alternative formulation of classical mechanics using radial distributions rather than instantaneous trajectories or orbital loci provide a conceptual link to corresponding formulations in quantum mechanics. This formulation has the advantage of permitting macroscopic and microscopic systems to be treated in an analogous manner, and provides a means of considering many-body systems through the use of numerical calculations.

Appendix A. Legendre functions of half-odd-integer order

Legendre functions of half-odd-integer order can be evaluated using the hypergeometric series

$$P_{-\nu-1}(z) = P_{\nu}(z) = \left(\frac{1+z}{2}\right)^{\nu} F\left(-\nu, -\nu; 1; \frac{z-1}{z+1}\right). \quad (\text{A.1})$$

Thus

$$\langle r^k \rangle = \left(\frac{a+b}{2}\right)^k F\left(-\frac{k}{2}, -\frac{k}{2}; 1; \left(\frac{a-b}{a+b}\right)^2\right). \quad (\text{A.2})$$

For the case shown in the figures, $b = a/2$, this gives for the first moment,

$$\langle r \rangle = \frac{3a}{4} F\left(-\frac{1}{2}, -\frac{1}{2}; 1; \frac{1}{9}\right) = 0.77098a. \quad (\text{A.3})$$

In the limit $b \rightarrow 0$ we can use the fact that $F(a, a, ; c; 1) = \Gamma(c)\Gamma(c-2a)/\Gamma(c-a)^2$ to write the moments ($k \geq 0$) for a linear oscillator in one dimension:

$$\langle r^k \rangle_{1D} = \frac{k!a^k}{2^k \Gamma(1+k/2)^2}. \quad (\text{A.4})$$

These results check against the elementary results, for example

$$\langle r \rangle_{1D} = 2a/\pi, \quad \langle r^2 \rangle_{1D} = a^2/2, \quad \langle r^4 \rangle_{1D} = 3a^4/8. \quad (\text{A.5})$$

References

- [1] Curtis L J 2003 *Atomic Structure and Lifetimes: A Conceptual Approach* (Cambridge: Cambridge University Press)
- [2] Curtis L J and Silbar R R 1984 Self-consistent potentials for complex atoms: a semiclassical approach *J. Phys. B: At. Mol. Phys.* **17** 4087–101
- [3] Curtis L J, Haar R R and Kummer M 1987 An expectation value formulation of the perturbed Kepler problem *Am. J. Phys.* **55** 627–31
- [4] Eisberg R and Resnick R 1985 *Quantum Physics of Atoms, Molecules, Solids, Nuclei, and Particles* 2nd edn (New York: Wiley) pp 136–39
- [5] Sivadrière J 1989 Laplace vectors for the harmonic oscillator *Am. J. Phys.* **57** 524–5
- [6] Gradshteyn I S and Ryzhik I M 1965 *Tables of Integrals, Series and Products* (New York: Academic) formulae 3.661-3 and 3.661-4
- [7] Goldstein H 1980 *Classical Mechanics* 2nd edn (Reading, MA: Addison-Wesley)
- [8] Curtis L J and Ellis D G 2004 Use of the Einstein–Brillouin–Keller action quantization *Am. J. Phys.* **72** 1521–3